

Alternating spin splitting of electronic and magnon bands in two-dimensional altermagnetic materials

Qian Wang(王乾), Da-Wei Wu(邬大为), Guang-Hua Guo(郭光华), Meng-Qiu Long(龙孟秋), and Yun-Peng Wang(王云鹏)

Citation: Chin. Phys. B, 2024, 33 (**9**): 097507. DOI: 10.1088/1674-1056/ad6425
Journal homepage: http://cpb.iphy.ac.cn; http://iopscience.iop.org/cpb

What follows is a list of articles you may be interested in

First-principles study of electronic and magnetic properties of Fe atoms on $Cu_2N/Cu(100)$

Jiale Chen(陈佳乐) and Jun Hu(胡军)
Chin. Phys. B, 2024, 33 (**8**): 087502. DOI: 10.1088/1674-1056/ad5275

Spin gap in quasi-one-dimensional S=3/2 antiferromagnet $CoTi_2O_5$

Hao-Hang Xu(徐浩航), Qing-Yuan Liu(刘庆元), Chao Xin(辛潮), Qin-Xin Shen(申沁鑫), Jun Luo(罗军), Rui Zhou(周睿), Jin-Guang Cheng(程金光), Jian Liu(刘健), Ling-Ling Tao(陶玲玲), Zhi-Guo Liu(刘志国), Ming-Xue Huo(霍明学), Xian-Jie Wang(王先杰), and Yu Sui(隋郁)
Chin. Phys. B, 2024, 33 (**3**): 037505. DOI: 10.1088/1674-1056/ad1381

Oscillation of Dzyaloshinskii-Moriya interaction driven by weak electric fields

Runze Chen(陈润泽), Anni Cao(曹安妮), Xinran Wang(王馨苒), Yang Liu(柳洋), Hongxin Yang(杨洪新), and Weisheng Zhao(赵巍胜)
Chin. Phys. B, 2024, 33 (**2**): 027501. DOI: 10.1088/1674-1056/ad0f85

Stacking-dependent exchange bias in two-dimensional ferromagnetic/antiferromagnetic bilayers

Huiping Li(李慧平), Shuaiwei Pan(潘帅唯), Zhe Wang(王喆), Bin Xiang(向斌), and Wenguang Zhu(朱文光)
Chin. Phys. B, 2024, 33 (**1**): 017504. DOI: 10.1088/1674-1056/ad053d

Controllable high Curie temperature through 5d transition metal atom doping in CrI_3

Xuebing Peng(彭雪兵), Mingsu Si(司明苏), and Daqiang Gao(高大强)
Chin. Phys. B, 2024, 33 (**1**): 017503. DOI: 10.1088/1674-1056/ad053b

---

RAPID COMMUNICATION

Alternating spin splitting of electronic and magnon bands in two-dimensional altermagnetic materials

Qian Wang(王乾), Da-Wei Wu(邬大为), Guang-Hua Guo(郭光华), Meng-Qiu Long(龙孟秋)†, and Yun-Peng Wang(王云鹏)‡

School of Physics, Central South University, Changsha 410083, *China*

(Received 27 June 2024; revised manuscript received 16 July 2024; accepted manuscript online 17 July 2024)

Unconventional antiferromagnetism dubbed as altermagnetism was first discovered in rutile structured magnets, which is featured by spin splitting even without the spin–orbital coupling effect. This interesting phenomenon has been discovered in more altermagnetic materials. In this work, we explore two-dimensional altermagnetic materials by studying two series of two-dimensional magnets, including MF_4 with M covering all 3d and 4d transition metal elements, as well as TS_2 with T = V, Cr, Mn, Fe. Through the magnetic symmetry operation of RuF_4 and MnS_2, it is verified that breaking the time inversion is a necessary condition for spin splitting. Based on symmetry analysis and first-principles calculations, we find that the electronic bands and magnon dispersion experience alternating spin splitting along the same path. This work paves the way for exploring altermagnetism in two-dimensional materials.

Keywords: two-dimensional altermagnetic materials, altermagnetism, spin splitting, first-principles calculations

PACS: 75.50.Ee, 61.50.Ah, 11.55.Fv **DOI:** 10.1088/1674-1056/ad6425

1. Introduction

Antiferromagnetic materials have received widespread attention due to their scalability and high stability against magnetic field disturbances. Unlike ferromagnetic materials with all local magnetic moments pointing along the same direction,[1,2] antiferromagnetic materials possess alternating local magnetic moments at different magnetic atomic sites compensating with each other, so the net magnetization is zero.[3–6] The electronic states in conventional antiferromagnetic materials exhibit no spin polarization anywhere within the reciprocal space. The electronic energy band is thus spin degenerate and preserves the time-reversal symmetry if one neglects the spin–orbital coupling (SOC). Recently, unconventional antiferromagnetism was discovered in rutile-structured magnets with collinear compensated magnetism. The time-reversal symmetry is broken in these materials and the electronic structure exhibits momentum-dependent spin splitting even without considering the SOC, which is different from the conventional antiferromagnetism. This new unconventional antiferromagnetic phase is referred to as the altermagnetism.[7–9]

The altermagnet can be viewed as two interpenetrating ferromagnets with opposite magnetizations that generates spin-splitted Fermi surface due to the local anisotropy in the crystal potential.[10] The spin splitting in collinear altermagnets within the non-relativistic regime was analyzed using the spin space group theory.[7,11–13] Analysis of the spin structure motif helps to provide geometric insights into the momentum dependence and the size of spin splitting.[14] The spin-splitted Fermi surface contributes to spin Seebeck[15–19] and spin Nernst effects.[20,21] The symmetry of the reciprocal spin order parameter would also be reflected in the spectra of spin waves and other spin-related quasi-particles. The two magnons with opposite chirality become non-degenerate because of the anisotropic exchange coupling.[22] The resulting longitudinal and transverse spin currents in antiferromagnetic insulators lead to spin thermal transport.[23]

A list of altermagnetic materials, including RuO_2, $MnTe_2$, RuF_4, Mn_3Sn, MnS_2, $LaMnO_3$ and many others, have been predicted using first-principles calculations.[7,8] Recently, the alternating spin splitting in $MnTe_2$ has been verified in experiments.[24,25] The altermagnetism in two-dimensional magnets has drawn special attention recently. Twist of non-altermagnetic bilayers leads to non-relativistic spin splitting.[26] Although spin splitting in altermagnetic materials has been found experimentally and theoretically, both the classification and the theoretical explanation of spin splitting in altermagnetic materials have been studied. However, the role of magnetic symmetry in spin splitting is not clear.

In this work, we explore the altermagnetism in two series of two-dimensional magnetic materials., namely, MF_4 with M ranging all 3d and 4d transition metals, and TS_2 with T = Cr, Fe, V, Mn. We study the electronic structure and the magnon dispersion using first-principles method. Without spin–orbital

†Corresponding author. E-mail: mqlong@csu.edu.cn
‡Corresponding author. E-mail: yunpengwang@csu.edu.cn

© 2024 Chinese Physical Society and IOP Publishing Ltd

coupling, we find that both the electronic energy band and magnon bands in RuF_4 and MnS_2 structures have spin splitting in the same Brillouin zone. Through the analysis of its symmetry, we elucidate the effects of twisting non-magnetic atoms and lattice symmetry on spin splitting.

2. Computational details

Density functional theory calculations were carried out using the Vienna *ab initio* simulation package (VASP)[27,28] and the OpenMX package.[29,30] In VASP calculations, we added Hubbard correction with $U_{\text{eff}} = 3$ eV for d-orbitals of transition metal ions.[31] We adopted the generalized gradient approximation of the exchange–correlation functional by Perdew, Burke, and Ernzerhof (PBE).[32] The electronic wave functions were expanded using the plane wave basis set with a kinetic energy cutoff of 500 eV. A uniform $5 \times 5 \times 1$ k-mesh was used for atomic structure relaxation until the residual forces on atoms smaller than 10^{-3} eV/Å. In OpenMX calculations, the electronic wave functions were expanded using pseudo atomic basis orbitals of Mn10.0-s3p3d3f1, S9.0-s3p3d2f1 and Ru7.0-s2p2d2f1, F6.0-s2p2d1. The energy cutoff was set to 230 eV, and no spin–orbital coupling effect was considered.

The magnetic interaction parameters were calculated using two different methods, namely, the four-states method[33] and the Green's function method.[34] We built $3 \times 3 \times 1$ supercells and calculated the total energies of different magnetic configurations and then fed them into the four-states method for extracting magnetic interaction parameters.[35–37] The TB2J Python package[34] implementing Green's function method along with OpenMX was also used for computing the magnetic interaction parameters between local magnetic moments. The TB2J approach is more computationally cheap and is more robust for materials with strong magnetic interactions. We calculated magnon dispersion using the results from TB2J.

3. Results and discussion

We have studied two different series of 2D antiferromagnetic materials. These materials are all square lattices, but those lattices' structure and symmetry are different. The first series is MF_4, with M ranging from 3d to 4d transition metals. DFT calculations predict that only RuF_4 and VF_4 exhibit spin splitting in their band structures, while CuF_4, PdF_4 and AgF_4 are ordinary antiferromagnetic metals. All other MF_4 materials are ordinary antiferromagnetic insulators with the spin-up bands overlapping with spin-down bands. The second series of materials studied in this work is TS_2 with T ranging from 3d to 4d transition metals. Our calculations show that FeS_2 and MnS_2 possess the antiferromagnetic phase as the ground state and exhibit altermagnetic band structures.

In the following, we only discuss results of RuF_4 and MnS_2 as representatives of the two series of 2D antiferromagnetic materials possessing altermagnetic properties. Based on their lattice structures, we employ the group theory to analyze the spin splitting in the electronic band structure and the splitting in magnon dispersion relation. Our DFT calculations reproduce the group theory results and confirm these two materials as altermagnetic 2D materials.

3.1. The atomic structure and lattice stability

Monolayer RuF_4 can be described using the space group of $P21/c$ (No. 14). Each primitive cell is composed of two Ru atoms and eight F atoms shown in Fig. 1(a). A Ru atom is surrounded by an octahedron formed by six nearest-neighboring F atoms. The Ru–F–Ru bond angle is 138°. The experimental lattice constants of bulk RuF_4 are $a = 5.6$ Å, $b = 4.95$ Å, and $c = 5.4$ Å.[38,39] The RuF_4 atomic layers are stacked along the [101] direction with van der Waals interaction between adjacent layers. Our DFT calculations predict lattice constants of $a = 5.43$ Å and $b = 5.2$ Å for the monolayer, in good agreement with the experimental data. The calculated local magnetic moment on each Ru ion is about 1.5 μ_B.[38]

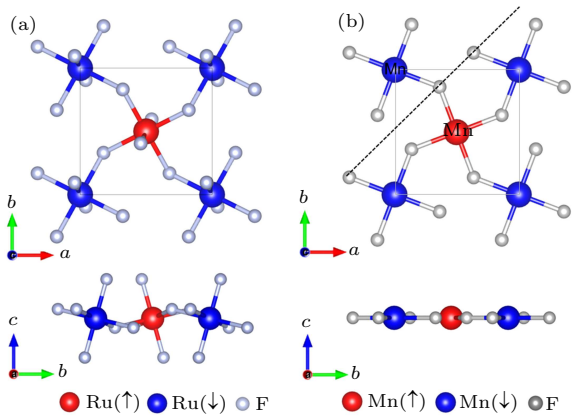


Fig. 1. (a) and (b) Top and side views of RuF_4 and MnS_2, respectively. The red atoms represent spin up and the blue atoms represent spin down.

MnS_2 has a different atomic structure from RuF_4. MnS_2 has a planar structure with two Mn atoms carrying opposite magnetic moments within its unit cell, see Fig. 1(b). Here the red atoms represent spin up and the blue atoms represent spin down. The crystal structure of MnS_2 can be described using the space group of $p4/mbm$ (#127), which is higher than that of RuF_4. The top view shows that two Mn ions and three S ions form a pentagon. The calculated local magnetic moment on each Mn ion is 2.7 μ_B, which is close to that of a nominal Mn^{4+} ion with 3 μ_B. The optimized lattice constant is 5.68 Å. The calculated phonon spectrum as shown in Fig. 2 exhibits no imaginary frequencies, confirming that the monolayer MnS_2 and RuF_4 are stable. Figure 2(c) shows the Brillouin zone of MnS_2 and RuF_4.

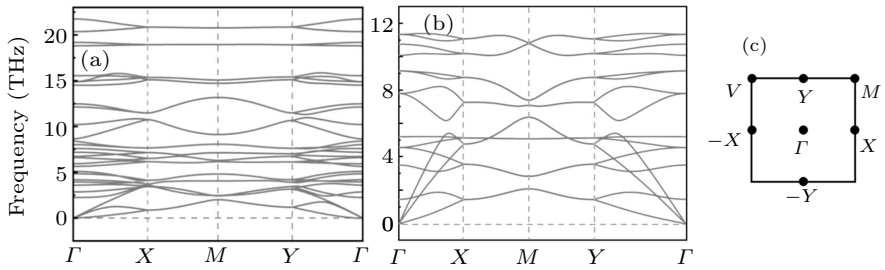


Fig. 2. The calculated phonon spectra of (a) RuF_4 and (b) MnS_2. (c) The first Brillouin zone of RuF_4 andMnS_2 and high-symmetric points.

3.2. Symmetry analysis

Before discussing the calculated band structure, we first carry out symmetry analysis on the spin splitting in the band structure. We ignore the spin–orbital coupling effects in the following analysis. In our study, we have adopted a unique system that treats the two spin channels as distinct colors, namely, black and white symmetry, as proposed by Lifshitz.[40] This conceptualization allows us to represent the magnetic atoms with opposing local magnetic moments through these contrasting colors. We denote a symmetry operation that swaps these colors as $\bar{T}$. It is important to note that this $\bar{T}$ operation is analogous to the standard time-reversal symmetry operation, but it crucially does not alter the wave vector. Instead, it focuses on the exchange of colors, which is a reflection of the spin channels. Our crystallographic operations are designed to affect only the spatial positions of the atoms, leaving the color (or spin state) of each atom unchanged. For example, the spatial-only mirror operation $\bar{M}$ transforms the spatial coordinates from (x,y) to (y,x) and the reciprocal space coordinates from (k_x,k_y) to (k_y,k_x). This operation is purely spatial and does not involve any change in the spin state. As illustrated in Fig. 1(b), the composite symmetry operation for the MnS_2 material involves a combination of $\bar{T}$ and $\bar{M}$ along the indicated dashed line. This combination encapsulates the symmetry properties of the material under investigation

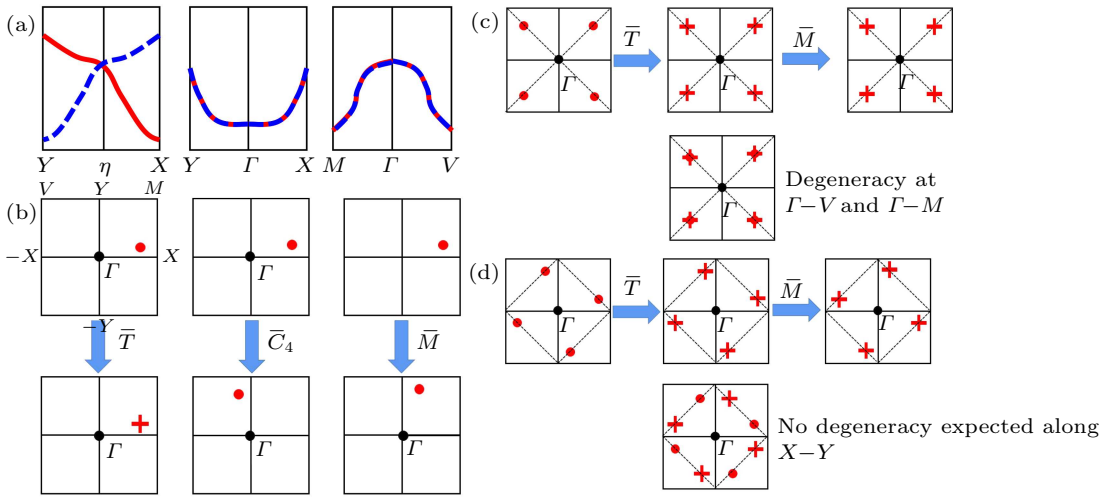


Fig. 3. (a) Schematics of the band structure of two-dimensional magnets with the same crystal symmetry as MnS_2, with red and blue indicating different spin bands, η is the midpoint of the X–Y path. (b) Effect of symmetry operations: $\bar{T}$ is the time reversal operation; $\bar{C}_4$ stands for the rotational operation by $\pi/2$; $\bar{M}$ represents a mirror operation in the [110] direction. The dots and crosses represent different spins. Under the combined time-reversal ($\bar{T}$) and mirror ($\bar{M}$) operations, no splitting occurs along the Γ–M and Γ–V paths (c), however, splitting occurs along the X–Y path (d).

We start from MnS_2 which has a higher symmetry. The rotations by 90°, 180°, and 270° around the out-of-plane direction transform the crystal to its original state shown in Fig. 3(b). Therefore, MnS_2 has a four-fold rotational symmetry. The group theory tells that the dispersions of electronic states, magnons, and other quasiparticles obey the crystal symmetry: $E(\boldsymbol{k}) = E(\bar{C}_4\boldsymbol{k})$, where $\boldsymbol{k}$ is a general point in the reciprocal space, $\bar{C}_4$ is the rotational operation by 90° and $E(\boldsymbol{k})$ is the quasiparticle energy at this $\boldsymbol{k}$-point. In the first Brillouin zone, the X-point is transformed to Y-point by rotation of 90°, and the M-point rotates to V-point. The group theory predicts that quasiparticle dispersions along the Γ–X and Γ–Y paths are degenerate, and so do the Γ–M and Γ–V paths. Because they have rotational and mirror symmetries.

If one ignores the spin of Mn ions, the spatial-only mirror operation with respect to the plane containing the out-of-plane direction and the [110] direction, we call it $\bar{M}$, is another symmetry operation. However, if one takes the spin into account, $\bar{M}$ is no longer a symmetry operation because it brings up-spin to down-spin and down-spin to up-spin. The $\bar{M}$ oper-

ation brings the X-point to the Y-point and Y to X. Therefore, the energy bands on the X–Y path are not spin-degenerate and possible to show spin splitting.

After the spatial-only mirror operation, one needs an analogous to the standard time reversal symmetry operation to return to the initial state ($\bar{T}$). So the combined operation $\bar{T}\bar{M}$ is a black and white symmetry operation. This fact results in the spin-degeneracy along the Γ–X, Γ–Y, Γ–M and Γ–V paths, see Fig. 3(c). From Fig. 3(d), one can see that the spin up (down) energies on the η–X path are equal to the spin down (up) energies on the η–Y path. Therefore, the dispersion along the X–Y path is symmetric with respect to its middle point η, but with opposite spin.

The RuF_4 monolayer has a lower symmetry than MnS_2, for the the two extra F anions upper and lower than the Ru atomic layer in RuF_4 are not directly above the Ru atom. Crystal symmetry analysis shows that under the combined two-fold rotation around the [010] direction and translation operation, the RuF_4 crystal returns to its original configuration. RuF_4 is short of four-fold rotational symmetry, which leads to additional band splitting along the Γ–M and X–Y paths.

3.3. Electronic and magnon dispersions

The calculated spin-resolved electronic band structure of MnS_2 monolayer is shown in Fig. 4(a). As expected from the above symmetry analysis, MnS_2 exhibits spin splitting in the electronic structure along the X–η–Y path. The energy of spin-up bands along the η–X path is identical to the spin-down bands along the η–Y path. The same band structure along Γ–X and along Γ–Y is the result of the four-fold rotational symmetry. These features in the calculated electronic structure agree with our previous symmetry analysis. The spin-splitting energy can reach as large as 0.24 eV along Γ–X and along Γ–Y, which is much larger than that in VF_4 of 50 meV.[41]

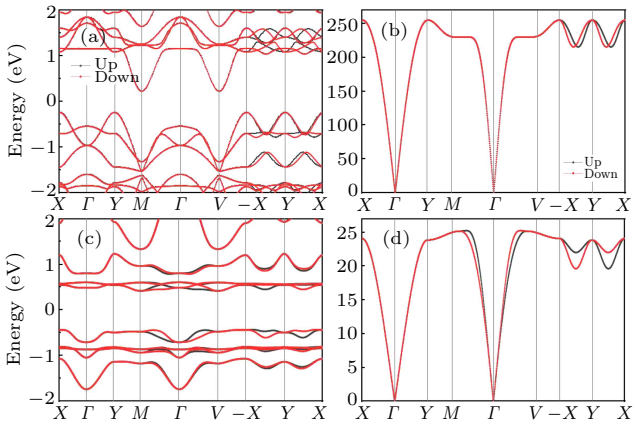


Fig. 4. (a) and (b) Band structure and magnetic dispersion of MnS_2. They both experience splitting on X–Y. (c) and (d) Band structure and magnetic dispersion of RuF_4. They exhibit splitting on X–Y and Γ–M.

We also calculated the dispersion of magnon in MnS_2 monolayer. The Heisenberg exchange interaction strength between local magnetic moments on Mn atoms was obtained using the TB2J code interfaced with OpenMX. The obtained values are $J_1 = 18$ meV, $J_2 = 0.1$ meV, $J_3 = -1.3$ meV, $J_4 = 0.23$ meV, $J_5 = -0.06$ meV, $J_6 = 0.28$ meV. The J_1 term refers to the exchange interaction with nearest neighboring Mn ions. The value J_1 is positive and its magnitude is much larger than the others, consistent with the antiferromagnetic ground state.

The meanings of other terms are illustrated in Fig. 5. The symmetry of MnS_2 crystal only allows distinct magnetic interactions among the seventh nearest neighbors. The J_7 and J_7^*, the magnetic interactions along the [–120] and [120] directions, respectively, have different values: $J_7 = -0.07$ and $J_7^* = 0.013$. Although the magnitudes of both J_7 and J_7^* are much smaller than that of J_1, they break the symmetry and lead to the splitting of magnon bands along the X–Y paths, as shown in Fig. 4(b). Comparing the electronic structure in Fig. 4(a), one can see that the splitting of electronic bands and magnon bands occurs along the same path.

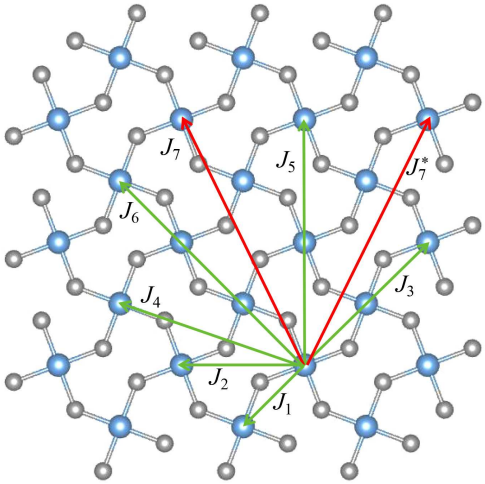


Fig. 5. The magnetic exchange interaction between different Mn atoms in MnS_2, where J_7 and J_7^* are not equal.

Next we discuss the calculated results of RuF_4 monolayer. Consistent with the above crystal symmetry analysis, the electronic bands show spin splitting along the X–Y path as the case of MnS_2; in addition spin splitting occurs also along the Γ–M path due to its lower symmetry than MnS_2.

The magnetic exchange interactions among Ru ions were calculated using the four-state energy mapping method. Using a $3 \times 3 \times 1$ supercell, we obtained $J_1 = 2.76$ meV and $J_2 = 0.30$ meV. The positive value of J_1 guarantees the antiferromagnetic ground state. Because of the lower symmetry, the exchange interactions with the third nearest neighbors already have two distinct values of $J_3 = 0.12$ meV and $J_3^* = 0.26$ meV. The calculated magnon dispersion relation using these magnetic exchange interactions is plotted in Fig. 4(d). The magnon bands split along the Γ–M and X–Y paths, exactly where the electronic band exhibits spin splitting.

4. Conclusion

In conclusion, we studied the altermagnetism in two series of two-dimensional magnetic materials, including MF_4 and TS_2. The spin splitting in the electronic structure and the splitting of magnon bands in RuF_4 and MnS_2 were analyzed in detail using the crystal symmetry and calculated using first-principles method. This work extends the investigation of altermagnetism to two-dimensional materials. The spin Seebeck effect refers to the spin voltage produced by the temperature gradient, which can be significantly influenced by the structure of the spin-polarized bands we find in the material. Similarly, spin energy effects, including the generation of transverse voltages in response to a temperature gradient, can also be modulated by the presence of a splitting band. These effects are crucial in the fields of spintronics and thermoelectricity, where manipulation of spin degrees of freedom can lead to new applications.

Acknowledgements

Project supported by the National Natural Science Foundation of China (Grant No. 12004439), Hunan Province Postgraduate Research and Innovation Project (Grant No. CX20230229), and the computational resources from the High Performance Computing Center of Central South University.

References

[1] Chumak A V, Vasyuchka V I, Serga A A and Hillebrands B 2015 *Nat. Phys.* **11** 453
[2] Wang Y P and Long M Q 2020 *Phys. Rev. B* **101** 024411
[3] Baltz V, Manchon A, Tsoi M, Moriyama T, Ono T and Tserkovnyak Y 2018 *Rev. Mod. Phys.* **90** 015005
[4] Cheng R, Xiao D and Zhu J G 2018 *Phys. Rev. Lett.* **121** 207202
[5] Zhou W, Zheng G, Li A, Zhang D and Ouyang F 2023 *Phys. Rev. B* **107** 035139
[6] Qi B T, Guo J J, Miao Y Q, Zhong M Z, Li B, Luo Z Y, Wang X G, Nie Y Z, Xia Q L and Guo G H 2022 *Frontiers in Physics* **10** 851838
[7] Šmejkal L, Sinova J and Jungwirth T 2022 *Phys. Rev. X* **12** 031042
[8] Šmejkal L, Sinova J and Jungwirth T 2022 *Phys. Rev. X* **12** 040501
[9] Yuan L D, Wang Z, Luo J W, Rashba E I and Zunger A 2020 *Phys. Rev. B* **102** 014422
[10] Yuan L D and Zunger A 2023 *Adv. Mater.* **35** 2211966
[11] Egorov S A, Litvin D B and Evarestov R A 2021 *J. Phys. Chem. C* **125** 16147
[12] Turek I 2022 *Phys. Rev. B* **106** 094432
[13] Fernandes R M, de Carvalho V S, Birol T and Pereira R G 2024 *Phys. Rev. B* **109** 024404
[14] Raghottam M S, Giuseppe C and Carmine A 2021 *Nanoscale* **15** 16998
[15] Li J, Shi Z, Ortiz V H, Aldosary M, Chen C, Aji V, Wei P and Shi J 2019 *Phys. Rev. Lett.* **122** 217204
[16] Wu S M, Zhang W, KC A, Borisov P, Pearson J E, Jiang J S, Lederman D, Hoffmann A and Bhattacharya A 2016 *Phys. Rev. Lett.* **116** 097204
[17] Uchida K, Xiao J, Adachi H, Ohe J, Takahashi S, Ieda J, Ota T, Kajiwara Y, Umezawa H, Kawai H, Bauer G E W, Maekawa S and Saitoh E 2010 *Nat. Mater.* **9** 894
[18] Shi Z, Xi Q, Li J, Li Y, Aldosary M, Xu Y, Zhou J, Zhou S M and Shi J 2021 *Phys. Rev. Lett.* **127** 277203
[19] Bai H, Zhang Y C, Zhou Y J, Chen P, Wan C H, Han L, Zhu W X, Liang S X, Su Y C, Han X F, Pan F and Song C 2023 *Phys. Rev. Lett.* **130** 216701
[20] Cheng R, Okamoto S and Xiao D 2016 *Phys. Rev. Lett.* **117** 217202
[21] Zyuzin V A and Kovalev A A 2016 *Phys. Rev. Lett.* **117** 217203
[22] Šmejkal L, Marmodoro A, Ahn K H, González-Hernández R, Turek I, Mankovsky S, Ebert H, D'Souza S W, Šipr O, Sinova J, *et al.* 2023 *Phys. Rev. Lett.* **131** 256703
[23] Cui Q, Zeng B, Cui P, Yu T and Yang H 2023 *Phys. Rev. B* **108** L180401
[24] Krempaský J, Šmejkal L, D'Souza S W, Hajlaoui M, Springholz G, Uhlířová K, Alarab F, Constantinou P C, Strocov V, Usanov D, Pudelko W R, González-Hernández R, Hellenes A B, Jansa Z, Reichlová H, Šobáň Z, Betancourt R D G, Wadley P, Sinova J, Kriegner D, Minár J, Dil J H and Jungwirth T 2024 *Nature* **626** 517
[25] Zhu Y P, Chen X, Liu X R, Liu Y, Liu P, Zha H, Qu G, Hong C, Li J, Jiang Z, Ma X M, Hao Y J, Zhu M Y, Liu W, Zeng M, Jayaram S, Lenger M, Ding J, Mo S, Tanaka K, Arita M, Liu Z, Ye M, Shen D, Wrachtrup J, Huang Y, He R H, Qiao S, Liu Q and Liu C 2024 *Nature* **626** 523
[26] He R, Wang D, Luo N, Zeng J, Chen K Q and Tang L M 2023 *Phys. Rev. Lett.* **130** 046401
[27] Kresse G and Hafner J 1993 *Phys. Rev. B* **47** 558
[28] Kresse G and Furthmüller J 1996 *Phys. Rev. B* **54** 11169
[29] Ozaki T 2003 *Phys. Rev. B* **67** 155108
[30] Ozaki T and Kino H 2005 *Phys. Rev. B* **72** 045121
[31] Wang H, Qi J and Qian X 2020 *Appl. Phys. Lett.* **117** 083102
[32] Liechtenstein A I, Anisimov V I and Zaanen J *Phys. Rev. B* **52** R5467
[33] Xiang H J, Kan E J, Wei S H, Whangbo M H and Gong X G 2011 *Phys. Rev. B* **84** 224429
[34] He X, Helbig N, Verstraete M J and Bousquet E 2021 *Computer Physics Communications* **264** 107938
[35] Xiang H, Lee C, Koo H J, Gong X and Whangbo M H 2013 *Dalton Trans.* **42** 823
[36] M-H, Whangbo, Koo H J and Dai D 2003 *J. Solid State Chem.* **176** 417
[37] Steenbock T and Herrmann C 2018 *Journal of Computational Chemistry* **39** 81
[38] Wang N, Chen J, Ding N, Zhang H, Dong S and Wang S S 2022 *Phys. Rev. B* **106** 064435
[39] Casteel W J J, Wilkinson A P, Borrmann H, Serfass R E and Bartlett N 1992 *Inorganic Chemistry* **31** 3124
[40] Lifshitz R 2004 arXiv preprint cond-mat/0406675
[41] Sodequist J and Olsen T 2024 *Appl. Phys. Lett.* **124** 182409